Acta Cryst. (1962). **15**, 1005

The Structure of Anorthite, $CaAl_2Si_2O_8$. I. Structure Analysis

By C. J. E. Kempster,* Helen D. Megaw and E. W. Radoslovich†

Crystallographic Laboratory, Cavendish Laboratory, Cambridge, England

(*Received* 5 *October* 1961 *and in revised form* 20 *November* 1961)

Anorthite $CaAl_2Si_2O_8$ has the same point group, $\bar{1}$, as a simple felspar, but four times the volume per lattice point; its unit cell is primitive, with a 14 Å *c*-axis, while that of albite, for comparison, is *C*-face-centred with a 7 Å *c*-axis. Anorthite approximates much more closely to a *C*-face-centred cell with a 14 Å *c*-axis than to either a body-centred cell with a 14 Å *c*-axis or a primitive cell with a 7 Å *c*-axis. The work was done in two stages. A synthesis using only main reflections gives elongated peaks or pairs of peaks whose centres of gravity define an 'average structure'. In the different subcells, atoms have displacements from the average positions whose magnitude and direction are given by the elongation (or 'splitting') and whose signs are found from the difference reflections (which also provide a check for magnitude and direction). The Ca peak has the most conspicuous elongation, and can be used for a heavy-atom method of determining the signs of the difference reflections. In the first stage, only '*c*'-type difference reflections were used, and the 14 Å *C*-face-centred approximation was obtained; a repeated application of the method using '*b*' and '*d*' reflections gave the true primitive structure. The final refinement was done by successive differential syntheses. Coordinates of the 52 independent atoms are given; their standard deviations are 0·0007 Å for Ca, 0·0015 Å for Si and Al, 0·0038 Å for O.

1. Introduction

1·1. *General approach*

Anorthite, $CaAl_2Si_2O_8$, is a member of the felspar family. The general features of the felspar structure have been known since the study of sanidine by Taylor (1933). Anorthite is one of the commonest and geologically most important members of the family, and it differs from the others in ways which made a detailed study desirable. Of the felspars whose structure has previously been studied, it is chemically most nearly related to celsian, $BaAl_2Si_2O_8$. Crystallographically, however, the triclinic symmetry and the radius of the large cation give it a closer resemblance to albite, $NaAlSi_3O_8$, and the significance of this relationship is strengthened by the occurrence of an apparently continuous series of solid solutions between the calcium and sodium felspars. It was therefore reasonable to take the structure of albite as a starting-point.

The obvious difference in chemical formula between anorthite and albite does not raise any difficulties in this approach. The scattering factors of Al and Si are so nearly identical that the difference between them could only become important at a very late stage of refinement. We write the felspar formula as AT_4O_8, *T* standing for 'tetrahedral cation', and make no attempt to distinguish the individual *T* cations as Si or Al during the analysis.

The present paper deals only with the method by which the structure was determined, the atomic coordinates found, and their accuracy. The description and discussion of the structure is left to a separate paper (Megaw, Kempster & Radoslovich, 1962). The nomenclature used throughout for the individual atoms is that proposed by Megaw (1956).

1·2. *Cell dimensions and lattice*

The cell dimensions of anorthite are given by Cole, Sørum & Taylor (1951); they are

$$a=8{\cdot}1768,\ b=12{\cdot}8768,\ c=14{\cdot}1690\ \text{Å};$$
$$\alpha=93°\ 10',\ \beta=115°\ 51',\ \gamma=91°\ 13'.$$

The *c*-axis is thus nearly double that of albite, the other dimensions being very similar. These authors also showed that anorthite has a primitive lattice, while albite is *C*-face-centred. This means that the asymmetric unit of anorthite is four times that of albite, the unit-cell content being 8 $CaAl_2Si_2O_8$. There is no evidence in the literature suggesting the absence of a centre of symmetry, and none arose in the course of this work. (The conclusions which can be drawn from the statistical distribution of intensities are discussed in § 2·3.) The space group is taken as $P\bar{1}$.

In reciprocal space, anorthite has four times as many lattice points as albite, classified for convenience as follows:

'*a*' type: $h+k$ even, l even
'*b*' type: $h+k$ odd, l odd
'*c*' type: $h+k$ even, l odd
'*d*' type: $h+k$ odd, l even.

Of these, only the '*a*' type correspond to possible reflections of albite. The rest, which arise from dif-

* Present address: Department of Physics, University of Adelaide, Adelaide, Australia.

† Present address: Division of Soils, Commonwealth Scientific and Industrial Research Organisation, Adelaide, Australia.

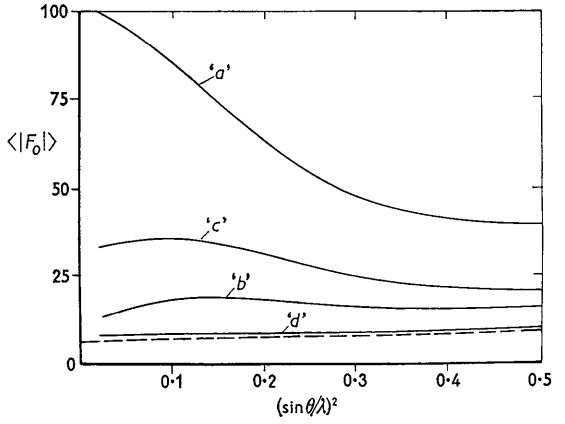

Fig. 1. Average non-zero $|F_o|$ values of four types of reflections, versus $(\sin\theta/\lambda)^2$. (The dashed line gives an estimate of the lowest experimentally observable value.)

ferences between the subcells, are on the whole very much weaker (see Fig. 1), indicating that the differences are small. The analysis of such a structure may be attempted by a method of successive approximations.

1·3. *Principle of method of solution*

It is easiest to understand the method of solution by considering a hypothetical structure with two subcells only. This is illustrated in Fig. 2(*a*), where $c/2$ is nearly but not exactly a translation vector, so that corresponding atoms in the two subcells are at slightly different positions, and the difference gives rise to weak reflections with odd l. A synthesis of reflections with even l will give a superposition of the two subcells, replacing each atom by two 'half atoms' (Fig. 2(*b*)), which in practice will probably appear as an unresolved elliptical peak (Fig. 2(*c*)). A synthesis of odd-l reflections (Fig. 2(*d*)) has to be added to this to reproduce the true structure. The mean parameters (x_m, y_m, z_m) give a reference point, shown by a dot, which is the same in each subcell. The difference parameters $\pm(\delta x, \delta y, \delta z)$ give the displacements of the actual atoms from this mean position. An illustration from the actual structure, corresponding to Figs. 2(*c*) and 2(*d*), is given in Fig. 7.

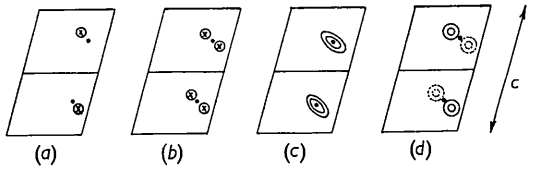

Fig. 2. Diagram illustrating effects in a hypothetical structure: (*a*) different atomic positions in two subcells, (*b*) 'average structure', showing positions of two 'half-atoms' in each subcell, (*c*) Fourier synthesis (F_o map) using main reflections, (*d*) Fourier synthesis (F_o map) using difference reflections. (Dotted lines show negative contours; contours in (*d*) are at smaller intervals than in (*c*).)

A knowledge of the approximate structure gives the signs of the even-l reflections only; hence the synthesis of Fig. 2(*c*) can be constructed, but not that of Fig. 2(*d*). From the former it is possible to deduce the mean position of the two half atoms and the magnitude of their separation or 'splitting' but not its sense, i.e. one cannot say which half atom belongs to which subcell. If there is only one 'split atom' the choice is arbitrary, but if there is more than one the question is a real one and can only be answered from the evidence of the difference intensities. The actual atomic parameters are the algebraic sum of the mean parameters and the difference parameters with correct sign. Once they are known the refinement of the structure as a whole can proceed in the ordinary way.

In principle the method is closely related to one used by Buerger (1956), but in detail the latter would have been inapplicable to our work even if we had known of it at an early stage (cf. Radoslovich, 1955). Buerger, concerned with differences of atomic *occupation* between subcells, takes the actual structure as made up of 'substructure' and 'complement structure', substructure being 'that part of the electron density which conforms to the substructure period'. We, concerned with differences of atomic *coordinates*, find a break-up into 'average structure' and 'difference structure' much more informative, even though the electron density over half the volume of the latter is necessarily represented as negative.

1·4. *Application to anorthite*

The above is a general method for structures with closely similar subcells. The determination of the signs of the difference parameters, however, remains an individual problem for each structure. One example occurred in the structure of celsian (Newnham & Megaw, 1960). In anorthite, there was the advantage that the Ca atoms were found experimentally to have the largest difference parameters, and hence a modification of the heavy-atom technique could be used. On the other hand, there was the disadvantage that the true structure had four subcells, not two, which meant that its derivation from that of albite had to proceed in two stages. Initially it was assumed that the first stage had been completed in Sørum's study of 'body-centred anorthite' (1951, 1953), and this structure was taken as the starting-point for the second stage. This soon proved not to be a good approximation, so a fresh approach was made. In this the average structure was referred to an albite-type subcell, and the strongest set of difference reflections, namely the '*c*' type (Fig. 1), was considered first, leaving the '*b*' and '*d*' types to be included at the second stage. This method proved successful, and the structure could finally be refined in the ordinary way using all four types of reflection.

It is convenient henceforward to refer to the set of difference parameters which would be zero if the '*c*' or the '*b*' reflections were systematically absent as the '*c*' *splittings* or the '*b*' *splittings* respectively.

Since this is a method of successive approximations, it is desirable to check its progress at every stage. This was done by considering not only the R-factor (which can be misleading) but also the height and shape of the peaks on Fourier maps, the amount of false detail in the background of F_o syntheses and difference syntheses, and the relative magnitude of the atomic shifts in successive syntheses. The continuous and simultaneous improvement in all these was evidence that the structure was refining truly.

2. Experimental

2·1. *Material*

The anorthite selected for analysis was from Monte Somma, Vesuvius (reference number B.M. 30744, provided by P. M. Game of the British Museum); it is from the same locality as the material (B.M. 49465) used by Taylor, Darbyshire & Strunz (1934) and Cole, Sørum & Taylor (1951). Gay (1953) points out that it is of low-temperature origin. Optical examination, using a universal-stage microscope, had shown its composition to be in the range 95–100% anorthite.

The material was found to be heavily twinned, but singly-twinned cleavage flakes could be picked out from crushed samples; by cutting with a sharp knife inside a small perspex box a few small untwinned blocks were obtained. The crystal finally chosen was of square cross-section, $0{\cdot}18\times0{\cdot}18\times0{\cdot}32$ mm., elongated roughly parallel to the a-axis.

The lattice constants were taken to be those of Cole, Sørum & Taylor (1951), which are quoted in § 1·2.

2·2. *Measurement of intensities*

Three-dimensional intensity data were collected from equi-inclination Weissenberg photographs, using filtered Mo $K\alpha$ radiation and the standard techniques of visual estimation with a comparison scale. Corrections were made for spot shape; in the later stages of refinement revised values were introduced, calculated by a modification of the method of Phillips (1954) (see Appendix). Some extinction effects were apparent for low-angle reflections; as suggested by Jellinek (1958) all reflections in these regions were omitted from difference syntheses, (and elsewhere replaced by calculated values), and not just the strongest ones with obvious discrepancies. Reflections in the central region of higher layers were also omitted, because for them the spot-shape correction was very large. In all, about 18% of the observed reflections were omitted.

No correction was made for absorption, because no convenient method was available. As a check, the absorption was calculated for a few selected low-angle reflections by the method of Albrecht (1939), and was found to vary from 19% to 37%. It was decided that these differences could be ignored, since accurate values of the temperature factors were not a primary object of investigation.

2·3. *General relations between observed intensities*

The final F_o and F_c values have been tabulated and can be made available on request.

The numbers and proportions of the four types of reflections are recorded in Table 1. Statistics are also included for a restricted group of strong structure factors (>60 on an absolute scale) comprising one quarter of the observed reflections. The difference reflections are evidently both weaker and less numerous than the main 'a' reflections, and the average intensities of the classes as a whole are in the order 'a' > 'c' > 'b' > 'd', irrespective of the distance from the origin of reciprocal space (Fig. 1).

It is clear that the structure of primitive anorthite approximates more closely to a base-centred (C-face-centred) structure than to a body-centred structure. This is a geometrical fact; the physical implications cannot be discussed till the structure as a whole is completely described.

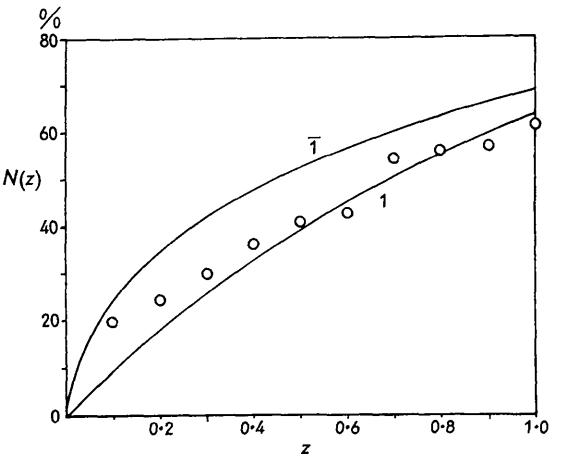

Fig. 3. $N(z)$ test applied to the 'a'-type $0kl$ reflections of anorthite.

Table 1. *Survey of anorthite structure factors*

Type of reflection	'a' $h+k$ even l even	'b' $h+k$ odd l odd	'c' $h+k$ even l odd	'd' $h+k$ odd l even	Total
No. observed	1346	478	853	114	2791
	48%	17%	31%	4%	
No. of strong reflections (>60 on absolute scale)	621	4	89	0	714
	87%	1%	12%	0	
Percentage of group below least observable	27%	71%	48%	93%	59%

The older statistical tests for the presence or absence of a centre of symmetry fail because of the large proportion of intensities below the observable limit, characteristic of this type of pseudosymmetric structure (see Table 1). If the $N(z)$ test is applied to the '*a*' reflections of the 0*kl* zone all but the first few points follow the acentric curve fairly closely (Fig. 3). This is probably due to the implicit assumption of an albite-size unit cell containing incompletely resolved quarter atoms, which is not in accordance with the random distribution of spherical atoms required by Wilson's (1949) theory. The $P(y)$ test (Ramachandran & Srinivasan, 1959), on the other hand, can and should be applied to *all* the reflections. When this is done, it speaks conclusively for centrosymmetry.

3. Outline of calculations

3·1. *Atomic scattering factors*

The scattering curves of Bragg & West (1928) were used in the early stages, but they were later replaced by others based on those of Berghuis, Haanappel, Potters, Loopstra, MacGillavry & Veenendaal (1955), modified by appropriate temperature factors (see § 3·2). An average between the curves for Al and Si was used throughout.

3·2. *Computing methods*

At the time when work on this structure was begun, no computer programme was available which was suitable for carrying out Fourier syntheses. Since it was clear that two-dimensional work would not give enough resolution, bounded projections were calculated (cf. Lipson & Cochran, 1953) using a Hollerith punched-card installation. It was thought initially that the unit cell would be covered adequately, without much overlap of atoms, by five slabs, bounded by the pairs of planes $x=0\pm\frac{1}{16}$, $x=\frac{1}{4}\pm\frac{1}{10}$, $y=0\pm\frac{1}{24}$, $y=\frac{1}{6}\pm\frac{1}{12}$, $y=\frac{1}{3}\pm\frac{1}{12}$. At a later stage thicker slabs with boundaries $x=0\pm\frac{1}{8}$, $x=\frac{1}{4}\pm\frac{1}{6}$, were found necessary.

Structure factors were computed on Edsac I.

When all the 52 independent atomic peaks had been individually located, difference syntheses in two and three dimensions were used for further refinement, calculated on Edsac I. The three-dimensional syntheses were computed in two stages, a set of generalized projections being calculated and used to give the coefficients for a series of one-dimensional syntheses scanning the whole volume. The electron-density differences near each atomic site were plotted out on a series of pieces of tracing paper representing parallel sections through the atom.

To calculate atomic shifts from the slopes in a difference synthesis it is necessary to know the curvatures of the peaks in the corresponding F_o synthesis, or to estimate these from their p-value and heights (Lipson & Cochran, 1953). The p-values are based on the assumption of a Gaussian atom, and to this approximation they are the same for the peaks in the bounded projections as in three dimensions, a fact which allows the peak height for the latter to be deduced from the former. The values adopted are given in Table 6(*c*).

Table 2. *Scattering factor coefficients*

Atom and state of ionization*	Scattering factor coefficients				
	A	*B*	*C*	*D*	*E*
Ca^{++}	5·590	1·697	8·061	13·042	4·259
Si^{++}/Al^{+}	7·612	2·857	2·249	63·642	2·128
O^{-}	4·463	7·056	3·035	36·845	1·478

* These 'states of ionization' were chosen arbitrarily, as being empirically reasonable. They make very little difference to F_c.

The final stages of refinement were done with a cyclic program on Edsac II (Wells, 1961). For this, the scattering factor curves of Berghuis *et al.* (1955) were fitted by expressions of the form

$$A\exp[-Bs^2]+C\exp[-Ds^2]+E\,,$$

(Forsyth & Wells, 1959). The coefficients (Table 2) were evaluated independently because of differences in the state of ionization assumed. The isotropic temperature factors were determined from two-dimensional syntheses and thereafter left unchanged.

After rejection of reflections liable to be in error because of extinction or spot shape, 2200 remained (82% of those observed). These F_o's were stored on magnetic tape. The F_c's were calculated, and the F_o's scaled to them by a single scaling factor not varying through reciprocal space. After calculation of an R-factor, reflections for which $||F_o|-|F_c||$ was greater than 10 on an absolute scale, or $|F_o|/|F_c|$ lay outside the range $\frac{1}{2}$ to 2, were tabulated and rejected; their number dropped from 70 at the beginning to 43 at the last cycle. The rest were used to calculate the values of differential syntheses at each atomic site, and the shifts, and new coordinates, were punched out as well as being fed back for a new cycle.

4. Structure analysis

4·1. *Preliminary work*

The first attempt used the structure of body-centred anorthite put forward by Sørum (1951) as a trial structure; the plan was to refine it, using '*a*' and '*b*' reflections, and then move to the true structure by including '*c*' and '*d*' reflections.

After two cycles of refinement, the Ca and *T* peaks were fairly clear and well defined; but the '*b*' splittings were much smaller than those determined by Sørum, and for some of the *T* peaks they differed in direction from his (though not by appreciably more than they changed in the course of his final three-dimensional refinement). The O peaks were irregular, of varying height, and as much as 1·5 Å from their expected positions. It seemed that some of them might have moved outside the limit of the bounded projections.

The Ca and T peaks were markedly elongated, as was expected because of the 'c' splittings. The magnitudes of these splittings were estimated from the peak contours by plotting out sections along the major and minor axes of the peaks; then if each atom has a cross section like that along the minor axis, the separation $2\delta r$ of two such atoms giving a cross section like that along the major axis can be found by trial.

Attempts were made to deduce the signs of the splittings, following which a synthesis gave fair agreement for Ca, but inconsistent results for T. It had become clear at this stage that the differences from Sørum's structure were too great to treat it as a reliable trial structure; if the magnitudes and directions of its 'b' splittings were not close to those of anorthite, their signs would be unreliable, and so would deductions about 'c' splittings which depended on them. This approach was therefore abandoned.

4·2. *Average structure from 'a' reflections*

The new approach started with a trial structure having an albitoid cell and thus giving 'a' reflections only. Their signs were assumed to be known fairly accurately from the preliminary work. A complete set of bounded projections was prepared; the layers at $x=0$ and $x=\frac{1}{4}$ are shown in Fig. 4.

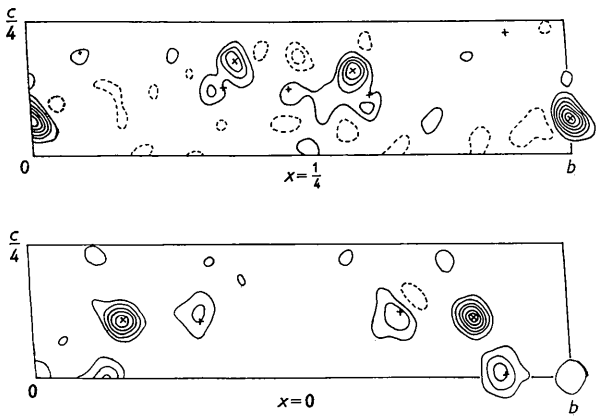

Fig. 4. First bounded projections: slabs at $x=0$ and $x=\frac{1}{4}$. Contours at intervals of 7·3 e.Å^{-3}; zero contour omitted. Cation peaks ×, anion peaks +. The strong peak near $(\frac{1}{4}, 0, 0)$ is Ca. The site of $O_D(m)$, which remained missing till a much later stage, is shown at the top right-hand corner of the slab at $x=\frac{1}{4}$.

As before, the Ca and T peaks were clear, the O peaks less good. Coordinates were obtained with fair accuracy for 11 of the 13 atoms in the asymmetric unit. The two remaining O's, $O_A(2)$ and $O_D(m)$, did not show up at all; positions were guessed for them in the gaps between the bounded projections.

Of the well-defined peaks the Ca appeared to show the largest splittings but some of the T peaks were also appreciably split.

Although each peak in this 'average structure' consists of four quarter atoms, it is necessary at this stage to assume that the 'b' splittings are negligible compared with the 'c' splittings, and so to treat each peak as if it were merely double. With the less important splittings this may give rise to indeterminacy or misinterpretation, but if the more important splittings are correctly interpreted ('important' in this context referring to the scattering factor of the atom concerned as well as the magnitude of the splitting) the errors may be expected to remedy themselves during refinement.

Since Ca, which has the largest splitting, is also the heaviest atom in the structure, it seemed likely that a 'heavy-splitting' method of solution might be effective. The fact that the difference reflections were observable as far out in reciprocal space as the 'a' type reflections agreed with the assumption that Ca made an important contribution to them. The criterion of the 'heaviness' of a heavy atom suggested by Lipson & Cochran (1953, p. 207) is the ratio $(\Sigma f^2)_{\text{heavy atoms}}/(\Sigma f^2)_{\text{other atoms}}$. For Ca in anorthite, using the Bragg–West scattering curves, this is 0·3 at low angles and 0·6 near the limit of visible reflections. If the ratio were 1·0, about 75% of all signs would be determined by the heavy atom. The effective 'heaviness' is expected to be enhanced by the large splitting.

4·3. *Location of symmetry centres*

In this first-stage reduction of symmetry, from 7 Å C-face-centred (albite-type) to 14 Å C-face-centred, half the centres of symmetry are lost, making it necessary to decide whether those retained are the set including (0, 0, 0) or the set including $(0, 0, \frac{1}{4})$ (referred to the 14 Å cell). The contribution of the Ca atoms must first be calculated for both possibilities.

The eight atoms which were originally equivalent in the double albite cell have now been divided into two sets of four, derived from atoms at

$$(x_m+\delta x, y_m+\delta y, z_m+\delta z) \quad \text{and}$$
$$(x_m-\delta x, y_m-\delta y, \tfrac{1}{2}+z_m-\delta z)$$

by the operation of the centre of symmetry and the C-face centring. Writing

$$\Theta = 2\pi(hx_m+ky_m+lz_m)$$
$$\Delta = 2\pi(h\delta x+k\delta y+l\delta z)$$

it can be shown that the structure factor contributions in the two cases are as follows:

centre of symmetry at (0, 0, 0):

'a' reflections $\quad 8f\cos\Theta\cos\Delta$,
'c' reflections $\quad 8f\sin\Theta\sin\Delta$;

centre of symmetry at $(0, 0, \frac{1}{4})$:

'a' reflections $\quad \pm 8f\cos\Theta\cos\Delta$,
'c' reflections $\quad \pm 8f\cos\Theta\sin\Delta$.

The total structure factor is obtained by summing terms of this form over all the atoms in an asymmetric

unit of albite. In this initial approximation, however, all except Ca are assumed to be negligible. Since Δ is small compared with Θ, the factor $\cos\Delta$ or $\sin\Delta$ varies slowly in reciprocal space, modulating the rapidly varying factor $\cos\Theta$ or $\sin\Theta$. The effect on the inner '*a*' reflections is very like that of a highly anisotropic temperature factor, and is independent of the choice of origin. The '*c*' reflections are modulated by the factor $\sin\Delta$, which is zero in a plane of reciprocal space normal to the direction of splitting, and on either side of it gives a set of parallel plane fringes with maxima at $\Delta = \pm\pi/2$. The magnitude of these reflections depends on either $\cos\Theta$ or $\sin\Theta$ as above.

This argument was used to determine the position of the centres of symmetry. Both Θ and Δ are calculable for every *hkl*. Since the contribution of atoms other than Ca is relatively more important at small reciprocal radii, low-angle reflections were at first excluded from the analysis, as were those for which $\sin\Delta$ was small. Division of the rest into two groups according to whether $|\sin\Theta|$ or $|\cos\Theta|$ was greater gave no significant difference of average intensity between the groups. Inspection of the strongest '*c*' reflections proved more informative, however. Of 73 which were stronger than the strongest '*b*' reflection, 59 had $|\sin\Theta| > |\cos\Theta|$, showing conclusively that the centre of symmetry was at (0, 0, 0)—a result confirmed by all subsequent work. It is interesting that this selective method succeeded when the comprehensive method including the larger sample failed.

4·4. *T splittings*

In the array of intensities of '*c*' reflections on the reciprocal lattice the strong intensities lay conspicuously on the fringes where $\sin\Delta_{Ca}$ had a maximum, but in patches consisting of from 2 to 5 strong reflections separated by weaker ones. These patches could often be identified as the intersection of fringes due to one or more *T* splittings with those due to the Ca splitting. Though the interpretation along these lines was not complete, it was sufficiently comprehensive to be very encouraging.

4·5. *Syntheses using 'a' and 'c' reflections*

The first synthesis of '*c*' reflections—a set of bounded projections—was constructed using only those of strongest intensity, about one eighth of the total number observed, with the signs determined from their Ca contributions. This 'partial-*c*' synthesis is illustrated in Fig. 5. The '*c*' splittings are here shown by a slope at the atomic position, which lies between a trough and a peak. The Ca splitting, of course, came out very strongly in the direction assumed in calculating signs. In addition, appreciable slopes appeared at many of the other peak sites. The general background was still fairly undulating.

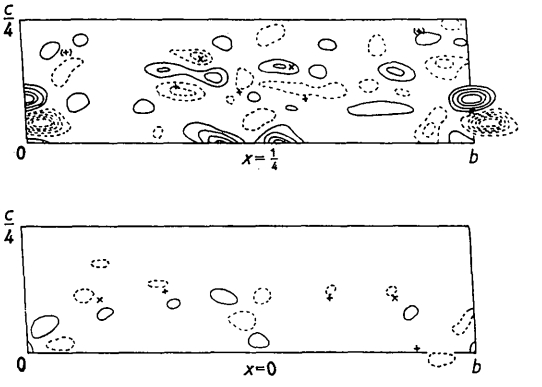

Fig. 5. 'Partial-*c*' synthesis, using only the strongest '*c*' reflections with signs determined by Ca. Diagram shows slabs of bounded projection at $x=0$ and $x=\frac{1}{4}$. Contours at intervals of 1·5 e.Å^{-3}; zero contour omitted; negative contours shown dotted. Cation peaks ×, anion peaks +. The peaks near $(\frac{1}{4}, \frac{1}{2}, 0)$ are false detail which disappears later.

This synthesis, by its construction, overemphasized the components of all splittings parallel to that of Ca. Better estimates of the magnitude and direction of the splittings were already available for some atoms from examination of the ellipticity of peaks in the synthesis of '*a*' reflections. The '*c*' synthesis, however, gave information about the signs of the difference parameters which could not be obtained from the '*a*' synthesis.

Table 3. *Proposed c-splittings for anorthite*

	Initial values			Refined values (at *C*-face-centred stage)		
Atom	δx	δy	δz	δx	δy	δz
Ca (000)	−0·0075	−0·0052	0·0058	−0·0020	−0·0174	0·0182
T_1 (0000)	0	0	0	−0·0055	0·0020	−0·0005
T_1 (*m*000)	0	0	0	−0·0018	0·0015	−0·0020
T_2 (0000)	−0·0071	−0·0031	−0·0028	−0·0076	0·0010	−0·0060
T_2 (*m*000)	−0·0057	−0·0015	0·0029	0·0032	0·0025	0·0065
O_A (1000)	0	0	0	0	−0·002	0·004
O_A (2000)	0·050	0	−0·017	0·001	0·003	0·001
O_B (0000)	0·004	−0·002	−0·004	−0·024	0·006	−0·018
O_B (*m*000)	0·025	−0·003	0·006	0·014	−0·011	0·002
O_C (0000)	0·003	0	−0·003	0·006	0	0·011
O_C (*m*000)	0	0	0	−0·020	0·001	0·002
O_D (0000)	−0·013	0·005	0·004	−0·008	0·003	0·011
O_D (*m*000)	0	0	0	0·020	0·012	−0·013

Two of the four T atoms now showed measurable splitting, as did five O atoms; for the other two T's the splitting was small and was taken as zero. The z parameters determined independently from the x and y projections agreed satisfactorily. The signs of the T splittings were checked by calculating their contributions to a number of F_c's corresponding to large F_o's. Where the Ca contribution was negligible, the T contributions were usually large; where both Ca and T contributions were large, they usually had the same sign. The difference parameters at this stage are recorded as 'initial values' in Table 3.

A second synthesis of the 'a' and 'c' reflections separately was constructed using the revised coordinates. All the peaks in the 'a'-reflection synthesis had improved, except $O_D(m)$ which was still missing. The 'c'-reflection synthesis (Fig. 6) showed much greater contrast between atomic sites and background, but was otherwise very much like the previous cycle, even at sites where it had been thought unsafe to attribute the slopes to splitting. This was satisfactory confirmation of the validity of the procedure. A further indication was provided by the behaviour (not illustrated in Fig. 6) of two oxygen atoms for which large splittings had been deduced: for $O_B(m)$ the splitting was confirmed, whereas for $O_A(2)$ it had disappeared, and in the 'a'-reflection synthesis the whole peak came up at one of the two 'half-atom' sites. It appeared that the mean position of this latter atom had been wrong by at least 0·5 Å in the earlier syntheses, and that it had not refined satisfactorily.

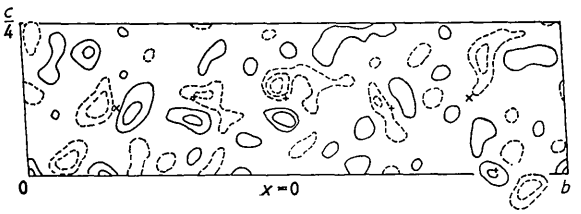

Fig. 6. First full 'c' synthesis. Diagram shows slab of bounded projection at $x=0$. Contours as in Fig. 5. Here the site of $O_A(2)$, near $(0, \frac{1}{2}, \frac{1}{8})$, is marked for the first time.

It seemed likely that the missing atom $O_D(m)$ was still misplaced by about 0·5 Å; a new position for it was proposed.

The sum and difference of the 'a' and 'c'-reflection syntheses were plotted for each peak, giving the electron density and atomic coordinates in the two subcells. Fig. 7 illustrates this procedure.

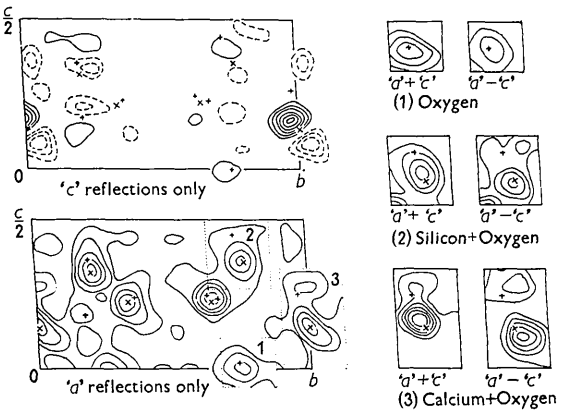

Fig. 7. Combination of 'a' and 'c' synthesis by sum and difference. Diagram shows projections on (100). Contours for 'a' at intervals of 6 e.Å^{-2}, zero and first contours omitted; contours for 'c' at intervals of 3 e.Å^{-2}, zero contour omitted. The small diagrams to the right show the effect of taking the correspondingly-numbered regions of the 'a' synthesis and adding or subtracting the electron densities in the same regions of the 'c' synthesis. Cation peaks ×, anion peaks +.

Here and throughout the analysis, adjustments to atomic coordinates were made from the evidence of the Fourier maps alone, and never from considerations of interatomic distance; the latter might have speeded up the refinement process, but might also have prejudged the bond lengths unwisely.

Next, several cycles of refinement were carried out using F_o, F_c, and (F_o-F_c) projections down the x-axis. (The y- and z-axis projections contained serious overlapping.) The R-factors at this and earlier stages are given in Table 4.

Table 4. *R-factors (as percentages)*

Where R-factors were calculated separately for different types of reflections, the types concerned are noted in the first column, and the separate values recorded in the later columns
From the stage illustrated in Fig. 9 onward, all types were taken together

Stage of work, and type of reflection used	*0kl*	*h0l*	*hk0*	Overall
After first 'a'+'c' bounded projections (Fig. 5): 'a', 'c'	53, 80	—	—	—
After refinement in projection: 'a', 'c'	31, 53	41, 51	45	—
After second 'a'+'c' bounded projections (Fig. 6): 'a'+'c'	32	37	34	—
After first determination of signs of 'b': 'a'+'c', 'b'	29, 50	—	—	—
After 'partial-b' (Fig. 8)	28·8	28·2	27·7	—
After final bounded projections (Fig. 9)	22·2	18·6	18·4	—
After two cycles of F_o-F_c projections	15·4	17·2	17·2	18·9
After first three-dimensional F_o-F_c synthesis	12·8	—	—	17·1
After second three-dimensional F_o-F_c synthesis	12·6	—	—	15·2
After revision of coordinates and F_o's	11·2	—	—	13·5, 12·4*
After 23 cycles of automatic refinement	9·6	—	—	(11·1), 10·2*

* These figures refer to about 82% of the reflections. The value in brackets is estimated for all reflections from the calculated value for the 82%.

Using the new coordinates of the 26 atoms, and taking '*a*' and '*c*' reflections together, a third set of bounded projections was calculated having the new limits $x=0\pm\frac{1}{8}$ and $x=\frac{1}{4}\pm\frac{1}{6}$. The general appearance was good, and the missing O atoms, $O_D(m000)$ and $O_D(m0ic)$, showed up for the first time, fairly close to their estimated positions. In estimating a new set of coordinates, rough corrections were made for the very pronounced diffraction effects.

The final difference parameters at the *C*-face-centred stage are given in Table 3. Most of them increased noticeably as the work progressed, but the x components in general decreased, though the peaks continued to show the marked elongation in the x direction which had led to the original high estimate of δx. This was clearly a diffraction effect, due to the distribution in reciprocal space of the observed data: the main collection of data was from photographs about the x axis, and layer lines with $h>8$ had not been included because of the extreme distortion of spot shape. Once recognized, this 'natural elongation' of the peaks could be allowed for, until it was eliminated by the use of difference maps.

4·6. *Second stage: inclusion of 'b' and 'd' reflections*

It had become clear towards the end of the first stage that one of the principal factors slowing down the refinement was failure to take account of the departures from the *C*-face-centred approximation, namely the '*b*' splittings of the 26 peaks. Replacement of each of these peaks by two half atoms is a possible first step in the second stage of the structure analysis. When this was done in the [100] projection it immediately reduced the *R*-factor by 5½%. This approach was not followed up because of programming difficulties.

An alternative approach started from the observation that one of the two Ca peaks, Ca (00), was considerably more elongated than any other, suggesting a repetition of the 'heavy-splitting' method applied to the '*b*' reflections. (The '*d*' reflections, which are few and weak, were omitted till the final stages.)

It was necessary, as previously, to begin by determining which of the two sets of symmetry centres in the *C*-face-centred approximation is retained as such in the true structure. An analysis like that of § 4·3 shows that the '*a*' and '*c*' structure amplitudes are the same for both choices, since $h+k$ is even, but that the '*b*' and '*d*' structure amplitudes are proportional to $\sin\Theta$ for a centre at (0, 0, 0), to $\cos\Theta$ for a centre at $(\frac{1}{4}, \frac{1}{4}, 0)$. Examination of 183 strong '*b*' reflections showed that 52% lay close to a maximum of $|\sin\Theta|$, 34% to a maximum of $|\cos\Theta|$. Further, of the 16 strong '*b*' reflections in the $0kl$ zone, 13 had large contributions from Ca if the centre of symmetry was at (0, 0, 0), and 8 if it was at $(\frac{1}{4}, \frac{1}{4}, 0)$. The centre was therefore tentatively placed at (0, 0, 0); the correctness of this choice was established by the successful refinement of the consequent trial structure.

There were now 13 strong '*b*' reflections in the $0kl$ zone whose signs were known from the Ca contribution, and these were used to construct a 'partial-b' x-axis projection. Only for the Ca atoms were the pairs of peaks related by '*c*' splittings sufficiently resolved in this projection to give clear information about the '*b*' splittings.

By assuming that strong '*b*' reflections arise when the contributions from Ca atoms and the rest of the framework are *both* strong and of the same sign, it was possible to allocate signs to the '*b*' splittings of six *T* peaks, their magnitudes being estimated from the final *C*-face-centred synthesis. (The splittings of the O peaks were too small for this.) The resulting set of difference parameters (Table 5) produced large contributions to all the 16 strong *b* reflections. A difference synthesis computed with these parameters was used to improve the coordinates of the four Ca atoms.

To check these conclusions, and to extend them to include the x-parameters, an independent estimate was made of the three-dimensional splittings for the atoms of the framework as described in § 4·5 for the '*c*' reflections. The contributions of the four Ca atoms were calculated for the 183 strong '*b*' reflections. Signs were indicated for 70% of these reflections, which were then used to construct a set of 'partial-*b*' bounded projections (Fig. 8). Comparison with the final bounded projections of the approximation using '*a*' and '*c*' reflections only—an approximation which now acts as an average structure—allowed splittings to be derived for

Table 5. *Proposed b-splittings for anorthite*

Atom	Values from x-projection		Values from first three-dimensional trial			Final values		
	δy	δz	δx	δy	δz	δx	δy	δz
Ca(000)	−0·011	0·008	−0·012	As in		0·0006	−0·0112	0·0066
Ca(*z*00)	−0·004	0·001	−0·005	x-projection		−0·0024	−0·0021	0·0008
T_1(0000)	0	0	0·004	−0·004	0	0·0056	−0·0046	−0·0041
T_1(0*z*00)	0·007	0·005	−0·004	0·004	0·002	0·0004	0·0021	0·0046
T_1(*m*000)	−0·007	0·006	0	−0·005	0·005	−0·0053	−0·0030	0·0050
T_1(*mz*00)	0·006	−0·008	0	0·005	−0·005	−0·0010	0	−0·0042
T_2(0000)	0·008	−0·004	0	0·007	0	0·0056	0·0036	0·0004
T_2(0*z*00)	−0·011	0	−0·003	−0·005	0	−0·0044	−0·0047	−0·0018
T_2(*m*000)	0·008	0·005	−0·002	0·003	0·001	−0·0058	0·0019	0·0033
T_2(*mz*00)	0	0	−0·003	−0·003	0	0·0020	0·0042	−0·0014

each of the eight T peaks; it also suggested possible splittings for several of the O peaks, which were however disregarded for the present. The difference parameters thus obtained agreed remarkably well with the two-dimensional set.

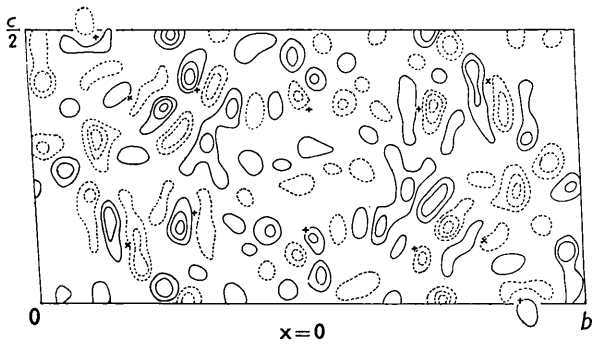

Fig. 8. Partial-b synthesis, using only the strongest b reflections, with signs determined by Ca. Diagram shows slab of bounded projection at $x=0$. Contours at intervals of 1·8 e.Å^{-3}, zero contour omitted. Cation peaks ×, anion peaks +.

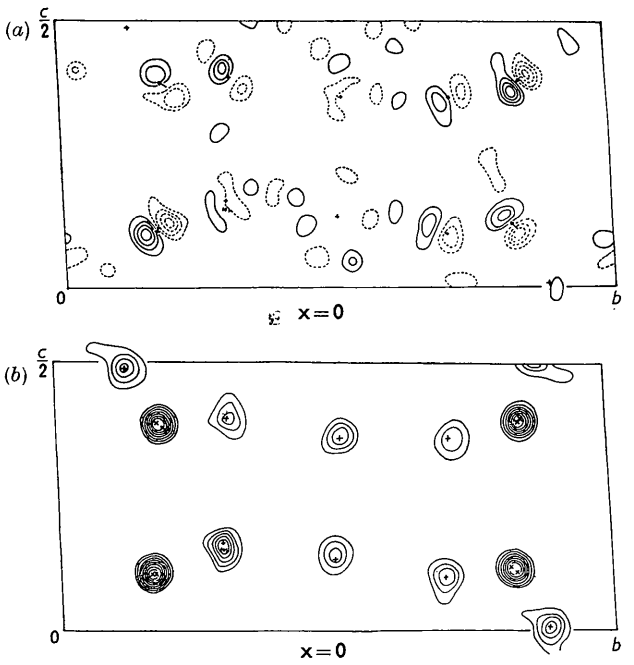

Fig. 9. (*a*) Final 'b'+'d' synthesis; contours at intervals of 1·8 e.Å^{-3}, zero contour omitted. (*b*) Final 'a'+'c' synthesis; contours at intervals of 8·3 e.Å^{-3}, zero contour omitted. Diagrams show slab of bounded projection at $x=0$. Compare with Fig. 4. Atoms marked × are T_1; atoms at $z=0, \frac{1}{2}$, are $O_A(1)$; atoms at $y=\frac{1}{2}$ are $O_A(2)$ (not visible in Fig. 4); the rest are O_C.

Combination of these difference parameters with the parameters of the C-face-centred approximation gave a trial structure with a primitive lattice.

A final set of bounded projections was calculated from the full set of observed reflections using this trial structure. Separate syntheses were constructed for the 'a' and 'c' reflections together, and the 'b' and 'd' reflections together. Both were greatly improved (Fig. 9); the ('b'+'d') synthesis was remarkably similar to the 'partial-b' synthesis at peak sites, but had a much tidier background elsewhere. In particular, several splittings of O atoms suggested by the earlier synthesis but not adopted in the trial structure reappeared in the new synthesis—an effect similar to that observed with the 'c' splittings (§ 4·5). It seems that deductions from the partial syntheses were too cautious—an error on the right side in a structure of this complexity—and that the use of the Ca splitting as a 'heavy splitting', analogous to that of a heavy atom, has been fully justified.

A synthesis of the complete structure was obtained by combining the ('a'+'c') and ('b'+'d') syntheses, and this gave new coordinates for all the atoms, including all the O's. The 'b' splittings for Ca were smaller than in the trial structure, the Ca peaks remaining somewhat elongated. The R-factors were much improved, but the calculated intensities of 'b' and 'd' reflections were still lower than the observed. There was very considerable scatter of bond lengths within the tetrahedra, making it impossible to detect any kind of Si/Al ordering. Nevertheless one could be confident that the structure was essentially correct and only needed refinement.

5. Refinement

5·1. *Use of difference syntheses*

Difference syntheses for the three cardinal projections were now so much improved that it was worth while using them for refinement while preparations were being made for three-dimensional syntheses. Certain interesting effects were noticed.

Two cycles of refinement of the x-axis projections

Table 6

(*a*) Isotropic temperature factors

	B values in Å^2		
Atom	Effective value in Bragg–West curves	First revised values from refinement of x-projection	Final values
Ca	0·4	1·0	1·0, 0·3
T	0·3	0·3	0·2
O	1·5	0·7	0·6

(*b*) Principal axes of thermal ellipsoids (direction of long axis is close to [110])

Ca(000)	0·75	1·88	0·32
Ca(zi0)	1·00	2·00	0·50
Ca(z0c)	0·40	1·18	0·50
Ca(0ic)	0·50	1·72	0·19

(*c*) p-values and peak heights

Atom	p	Peak height (e.Å^{-3})
Ca	7·2	80
T	8·3	67
O	6·8	28

Table 7. *Progress of refinement at various stages*

(*a*) Refinement by 3-dimensional ($F_o - F_c$) synthesis: Shifts in Å

		T		O	
	Ca	Mean	Max.	Mean	Max.
First cycle	Very small	0·021	0·039	0·046	0·085
Second cycle	Very small	0·012	0·021	0·028	0·048

(*b*) Automatic refinement programme

(δx, δy, δz are in fractions of cell edge $\times 10^4$)

	Calcium				I				O			
Cycle	δx	δy	δz	Shift (Å)	δx	δy	δz	Shift (Å)	δx	δy	δz	Shift (Å)
17	2·0	1·6	2·6	0·0046	3·8	1·9	1·9	0·0048	4·6	2·2	2·1	0·0056
18	1·4	1·4	1·9	0·0034	2·5	1·3	1·2	0·0031	3·1	1·8	1·5	0·0034
19	1·1	0·9	1·3	0·0023	2·1	0·9	0·7	0·0023	2·5	1·4	1·3	0·0032
20									2·0	1·3	1·1	0·0028
21									1·4	0·9	0·9	0·0021

reduced the *R*-factor from 22·2% to 15·4%; the '*b*' splittings for Ca increased towards their original values, the Ca peaks meanwhile becoming rounder; and the calculated intensities of '*b*' reflections increased. On all these points, therefore, the first complete F_o synthesis had been misleading, simply because more than 70% of the '*b*' and more than 90% of the '*d*' reflections were too weak to observe (Table 1). The omission of so many reflections from the ('*b*'+'*d*') synthesis meant that the observed slopes at the peak sites were lower than they should have been, and the deduced splittings therefore smaller. From this point onward, therefore, it was necessary to work with difference syntheses, even in three dimensions.

The first three-dimensional synthesis improved the coordinates but showed the inadequacy of the temperature factors implicit in the Bragg–West scattering factors. Revised values (Table 6) were obtained from two-dimensional work. A second three-dimensional synthesis gave further changes of atomic coordinates (Table 7(*a*)). The temperature factors were still not perfect, and the Ca peaks showed slight elongation, in a direction quite different from the previous splittings, but approximately the same for all four Ca's.

5·2. *Final refinement*

For final refinement, new spot-shape corrections (see Appendix) were used to give an improved set of F_o's. New techniques of computation had also become available.

An improved set of temperature factors was derived from two-dimensional data as follows. First the magnitudes of all temperature factors were adjusted till the scaling factor was constant and independent of reciprocal-space radius. Then their relative values were altered in a series of $F_o - F_c$ syntheses in the usual way. The two pairs of Ca peaks seemed to need quite different isotropic (mean) temperature factors, though all four peaks appeared to have the same elliptical shape, as judged from the *x*-axis and *y*-axis projections. These projections were used to estimate the lengths and orientations of the principal axes of the thermal ellipsoids (Table 6). The longest axis is roughly in the [110] direction for all four atoms. No three-dimensional refinements of these anisotropic effects has been attempted; more detailed examination of absorption effects would be needed before they can be taken as real.

Re-examination of the second three-dimensional synthesis suggested alterations in the coordinates of some of the O atoms. These lay at positions of moderate slope, but near regions of much steeper slope in the *x*-direction (the direction of slowest refinement). In the first interpretation of this synthesis, the shifts had been calculated from the slopes in the immediate environment of the atoms; the revised shifts were larger. It was noticed that this improved the regularity of *T*–O distances within the same tetrahedron; indeed, in some cases it was irregularities in the bond distances which called attention to the significance of features of the difference map, though irregularities were never by themselves used as criteria for shifting atoms.

These changes, together with the introduction of corrected F_o's, reduced the *R*-factor from 15·2% to 13·5%.

The revised coordinates and temperature factors were used as a starting point for the automatic refinement on Edsac II. The *R*-factor for the reflections actually used (cf. § 2·2) fell after 23 cycles from 12·4% to 10·2%, which probably corresponds to about 11·1% for the total number of observed intensities. The mean atomic shifts during the later cycles are recorded in Table 7(*b*), and the final coordinates in Table 8.

6. Errors

The errors in the coordinates were calculated using Cruickshank's formula (Lipson & Cochran (1953), equation 308·2). The curvature C_n, which appears in this formula, was calculated from the theoretical *f*-curve for the atom in question, modified by the

Table 8. *Final coordinates*

(In fractions of cell edge $\times 10^4$)

Atom	x	y	z	Atom	x	y	z
$O_A(1000)$	0276	1234	9957	$T_1(0000)$	0099	1584	1043
$O_A(1z00)$	9814	1237	4808	$T_1(0z00)$	0069	1609	6125
$O_A(10i0)$	4873	6256	4865	$T_1(00i0)$	5061	6567	6033
$O_A(1zi0)$	5129	6256	9970	$T_1(0zi0)$	4987	6675	1125
$O_A(2000)$	5724	9909	1451	$T_1(m000)$	9928	8146	1190
$O_A(2z00)$	5732	9901	6398	$T_1(mz00)$	0059	8154	6129
$O_A(20i0)$	0732	4876	6330	$T_1(m0i0)$	5078	3154	6212
$O_A(2zi0)$	0755	4925	1363	$T_1(mzi0)$	5034	3207	1091
$O_B(0000)$	8114	1027	0792	$T_2(0000)$	6841	1134	1512
$O_B(0z00)$	8071	0996	6046	$T_2(0z00)$	6818	1029	6644
$O_B(00i0)$	3363	5938	6045	$T_2(00i0)$	1906	6123	6681
$O_B(0zi0)$	2912	6036	0819	$T_2(0zi0)$	1714	6062	1504
$O_B(m000)$	8148	8516	1454	$T_2(m000)$	6749	8828	1881
$O_B(mz00)$	8090	8510	6018	$T_2(mz00)$	6799	8717	6715
$O_B(m0i0)$	2983	3575	6113	$T_2(m0i0)$	1759	3802	6744
$O_B(mzi0)$	3382	3606	1309	$T_2(mzi0)$	1865	3790	1815
$O_C(0000)$	0120	2780	1351				
$O_C(0z00)$	0177	2900	6486				
$O_C(00i0)$	5082	7778	6311				
$O_C(0zi0)$	5102	7969	1500				
$O_C(m000)$	0004	6802	1063	Ca(000)	2647	9844	0873
$O_C(mz00)$	0083	6898	6017	Ca(z00)	2684	0312	5438
$O_C(m0i0)$	5150	1794	6090	Ca(0i0)	7732	5354	5422
$O_C(mzi0)$	5067	1947	0974	Ca(zi0)	7636	5067	0740
$O_D(0000)$	1795	1072	1919				
$O_D(0z00)$	2153	1057	6862				
$O_D(00i0)$	6992	6031	6779				
$O_D(0zi0)$	6921	6014	2000				
$O_D(m000)$	2027	8723	2106				
$O_D(mz00)$	1754	8557	7170				
$O_D(m0i0)$	6861	3637	7335				
$O_D(mzi0)$	6999	3691	1993				

appropriate temperature factor, and by a cut-off in reciprocal space at the same radius as for the summation over the F's. The values of $\sigma(x_n)$ so obtained were: for Ca, 0·0007 Å; for T, 0·0015 Å; for O, 0·0038 Å. The dangers of accepting these values as trustworthy are: (i) that the method is reliable only when refinement is complete, and provides no internal check to show that this is so; (ii) that the curvatures are calculated, not derived empirically from the F_o map, and since they are very sensitive to cut-off radius they could be seriously over-estimated.

It is however possible to check the error estimate by examining the progress of refinement. If it goes smoothly, the atomic shifts should become progressively smaller; and the completion of refinement will be marked by shifts of steady r.m.s. value whose signs tend to reverse as the atoms move at random over the small volume characteristic of the random errors. If refinement is incomplete, it will depend on the program whether the atom approaches its final position steadily from one direction or by bracketing it. In the latter case, the r.m.s. value of the shifts provides an estimate of accuracy which allows for incomplete refinement. It can, however, only be safely used if it is clear that the shifts are reversing in sign; unless this is tested, there is a danger that the program may be providing too slow an advance to the final position to allow extrapolation.

Table 7(b) shows that the shifts of atomic positions are becoming small, but provides no test of their signs. In practice it was easier to examine the changes in T–O bond lengths rather than atomic coordinates. Before considering these changes some preliminary comments on the bond lengths are needed.

It was apparent from an early stage of the structure determination that the tetrahedra fell into two groups of unequal size. Though it was obvious that these must contain different proportions of Si and Al, this fact was never used at any time during the refinement; here, therefore, we shall simply distinguish the groups by the subscripts S (small) and L (large). Table 9 gives the variation of the mean bond length of each group, and their difference, in the final stages of refinement. The steady increase of the difference is very striking, and provides evidence that the refinement is meaningful. It is not safe to assume that all the bonds within a tetrahedron are equal, nor that all tetrahedral means within a group are equal. Nevertheless it is of interest to notice (Table 9) that their r.m.s. deviation from the tetrahedral mean and the group mean respectively drop during refinement until a very late stage, when they level off.

Table 9. *Refinement of T–O bond lengths, in* Å

Cycle	Mean bond length T_S–O	Mean bond length T_L–O	Difference	R.m.s. deviation from tetrahedral mean S	R.m.s. deviation from tetrahedral mean L	R.m.s. deviation of tetrahedral mean from group mean S	R.m.s. deviation of tetrahedral mean from group mean L	R.m.s. change of individual bond lengths S	R.m.s. change of individual bond lengths L
*A*1	1·635	1·720	0·085	0·044	0·062	0·024	0·013		
*B*1	1·626	1·729	0·103	0·036	0·053	0·023	0·016	0·014	0·014
14	1·622	1·739	0·117	0·028	0·046	0·019	0·009	0·021	0·020
21	1·616	1·746	0·130	0·029	0·042	0·009	0·005	0·015	0·016
22	1·615	1·748	0·133	0·030	0·042	0·008	0·005	0·007	0·008
24	1·614	1·749	0·135	0·026	0·036	0·008	0·006	0·0045	0·0041

Table 10. *Changes of bond length with* (1) *same sign*, (2) *opposite sign, in last two steps studied*

		(1)	(2)	Zero changes
No. of changes	*S*	12	17	3
	L	8	20	4
R.m.s. value of changes	*S*	0·0035 Å	0·0059 Å	
	L	0·0025 Å	0·0053 Å	

The r.m.s. changes of the individual bond lengths are recorded in the final column of Table 9; they appear to be approaching a steady low value. This is not by itself sufficient evidence to show that refinement is approaching completion, for the steps between the cycles recorded are not necessarily equal. However, Table 10 shows that the majority of the changes, particularly of the large ones, reverse sign between the last two cycles listed. Hence the atoms are oscillating about final positions; whether or not refinement is complete, the r.m.s. values of the changes estimate the overall error.

We may compare these final bond-length changes, 0·0045 Å and 0·0041 Å, with the error estimated from Cruickshank's formula, 0·0040 Å. The agreement is very satisfactory; even if its closeness is partly fortuitous, it suggests that the order of magnitude of the error estimate is trustworthy.

7. Discussion and summary

The lists of bond lengths and bond angles, and discussion of the structure itself, are left to Paper II.

Two principles have been used in solving the structure: (1) that omission of difference reflections in carrying out a Fourier synthesis is equivalent to averaging over those subcells which contribute to the difference reflections, (2) that the signs of difference reflections can be found by a heavy-atom technique. As a consequence of (1), the elongations of peaks on an F_o-map, or anomalies on a difference map, show the magnitudes of the difference parameters; as a consequence of (2), the difference reflections can be used to find the signs of the difference parameters (which must be opposite in the two subcells), and also, less accurately, to confirm the information about their magnitude. Because anorthite has four subcells, the whole process had to be repeated in two steps, the pairs of subcells that give rise to the stronger set of difference reflections being sorted out in the first step. It is essentially a method of successive approximations, and its progress can be, and has been, checked to make sure that no errors outside the permissible limits remain at any stage.

Since no assumptions about Si/Al distribution in the T sites, or about equality of T–O bonds within a tetrahedron or between tetrahedral means, have been made at any point in the analysis, the decrease in their r.m.s. deviations (Table 9) as refinement proceeds is independent evidence that no gross errors are being perpetuated. It can be seen, however, that differences within tetrahedra in the final structure are still rather large. The significance of these, and of differences between tetrahedral means and between groups of tetrahedra, will be discussed in Paper II.

We wish to record our thanks to Dr W. H. Taylor for suggesting this problem, and for constant help and encouragement during the work; to Dr P. Gay for advice and help in choosing the material; to Dr Wilkes and Mr Mutch for the facilities of the Mathematical Laboratory; to Mr M. Wells for devising the program for the final refinement; and to very many others who have helped with the computations over a period of years. One of us (C. J. E. K.) is indebted to the Department of Scientific and Industrial Research for a Maintenance Grant, and to the Nuffield Foundation for maintenance during the completion of the work; and one (E. W. R.) to the Commonwealth Scientific and Industrial Research Organisation for an Overseas Studentship.

APPENDIX

Correction for elongation and contraction of spots on higher layers was particularly important because, owing to the restricted range of the Weissenberg camera, many had been recorded on one side of the film only. Elongated and contracted reflections were handled separately. For layers $h=5$ and $h=6$, the ratio $\Sigma F_o/\Sigma F_c$ was evaluated over narrow annuli of reciprocal space, and plotted against the radius, ξ. The elongated reflections fitted the Phillips curves reasonably well; these curves were therefore used for all layers. The contracted reflections showed discrepancies; if they were fitted to the Phillips curves at

large ξ they diverged at small ξ. Hence empirical curves were drawn through the observed points, and from the curves for layers 5 and 6 those for the other layers were deduced. The corrected intensities for elongated and contracted reflections were scaled independently, layer by layer, to the calculated structure factors. When the same reflection occurred in both sets, agreement was good, and mean values were finally used.

References

ALBRECHT, G. (1939). *Rev. Sci. Instrum.* **10**, 221.

BERGHUIS, J., HAANAPPEL, IJ. M., POTTERS, M., LOOPSTRA, B. O., MACGILLAVRY, C. H. & VEENENDAAL, A. L. (1955). *Acta Cryst.* **8**, 478.

BRAGG, W. L. & WEST, J. (1930). *Phil. Mag.* **10**, 823.

BUERGER, M. J. (1956). *Proc. Nat. Acad. Sci. Wash.* **42**, 776.

COLE, W. F., SØRUM, H. & TAYLOR, W. H. (1951). *Acta Cryst.* **4**, 20.

FORSYTH, J. B. & WELLS, M. (1959). *Acta Cryst.* **12**, 412.

GAY, P. (1953). *Miner. Mag.* **30**, 169.

JELLINEK, F. (1958). *Acta Cryst.* **11**, 677.

LIPSON, H. & COCHRAN, W. (1953). *The Determination of Crystal Structures.* London: Bell.

MEGAW, H. D. (1956). *Acta Cryst.* **9**, 56.

MEGAW, H. D., KEMPSTER, C. J. E. & RADOSLOVICH, E. W. (1962). *Acta Cryst.* **15**, 1017.

NEWNHAM, R. E. & MEGAW, H. D. (1960). *Acta Cryst.* **13**, 303.

PHILLIPS, D. C. (1954). *Acta Cryst.* **7**, 746.

RADOSLOVICH, E. W. (1955). Thesis, Cambridge University.

RAMACHANDRAN, G. N. & SRINIVASAN, R. (1959). *Acta Cryst.* **12**, 410.

SØRUM, H. (1951). *K. Norske Vidensk. Selsk. Skr.* No. 3. Thesis, Trondheim.

SØRUM, H. (1953). *Acta Cryst.* **6**, 413.

TAYLOR, W. H. (1933). *Z. Kristallogr.* **85**, 425.

TAYLOR, W. H., DARBYSHIRE, J. A. & STRUNZ, H. (1934). *Z. Kristallogr.* **87**, 464.

WELLS, M. (1961). Thesis, Cambridge University.

WILSON, A. J. C. (1949). *Acta Cryst.* **2**, 318.

Acta Cryst. (1962). **15**, 1017

The Structure of Anorthite, $CaAl_2Si_2O_8$. II. Description and Discussion

BY HELEN D. MEGAW, C. J. E. KEMPSTER* AND E. W. RADOSLOVICH†

Crystallographic Laboratory, Cavendish Laboratory, Cambridge, England

(*Received* 5 *October* 1961 *and in revised form* 21 *November* 1961)

Anorthite has a felspar structure with the following particular features: (1) Si and Al tetrahedra alternate, so that each O atom has one Si and one Al neighbour; there is no Si/Al disorder. (2) Si–O and Al–O bond lengths show real variations within the same tetrahedron, the average value of each increasing as the number of Ca neighbours of the O atom increases from zero to 2. (3) There are 4 independent Ca atoms, 6- or 7-coordinated: pairs related (topologically, not exactly) by the *C*-face-centring translation have very similar environments, while those related by body-centring or by *z*-axis halving are very markedly different. There is no disorder of Ca position. (4) If the tetrahedra are grouped into the two topologically different types (distinguished conventionally by the subscripts 1 and 2 for their tetrahedral atoms) all tetrahedra of the same type have qualitatively similar bond-angle strains (i.e. departures from the tetrahedral angle of 109° 28′), independent of their Si/Al content. Comparison with other felspars shows that the strains are characteristic of the felspar structure, but are nearly twice as great in the felspars with divalent cations as in those with monovalent cations. (5) Most of the bond angles at O are in the range 125–145°, but there are some exceptionally large angles of about 165–170°.

These facts are explained by a model in which the building elements are nearest-neighbour bonds and bond angles, endowed with elastic moduli, acted on by the only unshielded cation–cation electrostatic repulsion, namely that acting across the centre of symmetry. The bond-angle strains at Si and Al are qualitatively predicted by it, and agree with observation. Most of the distortions of the felspar structure are common (qualitatively) to all felspars, depending on cation charge; others depend on cation size. In contrast to these, the effects of Si/Al distribution are relatively so small that discussion of them cannot usefully begin until the other larger effects have been clarified.

1. Introduction

Anorthite, $CaAl_2Si_2O_8$, is an important member of the felspar family. Other members of the family, whose structures have been determined in detail, and to which reference will be made here, are listed in Table 1. It was hoped that detailed comparison of the differences between members of the family would help our understanding not only of the felspars as a whole but also of the general character of three-dimensionally-linked framework structures. This has proved to be the case, as will be shown in what follows.

The method by which the structure was determined was described in Paper I (Kempster, Megaw &

* Present address: Department of Physics, University of Adelaide, Adelaide, Australia.

† Present address: Division of Soils, Commonwealth Scientific and Industrial Research Organisation, Adelaide, Australia.